Red-Shifted Cyanide Stretching Frequencies in Cyanide-Bridged Transition Metal Donor−Acceptor Complexes. Support for Vibronic Coupling

Murielle A. Watzky, John F. Endicott,* Xiaoqing Song, Yabin Lei, and Ariel Macatangay

Department of Chemistry, Wayne State University, Detroit, Michigan 48202-3489

Patterns in the cyanide stretching frequencies have been examined in several series of monometal- and CN^--bridged transition metal complexes. Metal-to-cyanide back-bonding can be identified as a major factor contributing to red shifts of ν_{CN} in monometal complexes. This effect is complicated in cyanide-bridged complexes in two ways: (a) when both metals can back-bond to cyanide, the net interaction is repulsive and results in a blue shift of ν_{CN}; and (b) when a donor and acceptor are bridged, ν_{CN} undergoes a substantial red shift (sometimes more than 60 cm^{-1} lower in energy than the parent monometal complex). These effects can be described by simple perturbational models for the electronic interactions. Monometal cyanide complexes and CN^--bridged back-bonding metals can be treated in terms of their perturbations of the CN^- π and π^* orbitals by using a simple, Hückel-like, three-center perturbational treatment of electronic interactions. However, bridged donor−acceptor pairs are best described by a vibronic model in which it is assumed that the extent of electronic delocalization is in equilibrium with variations of some nuclear coordinates. Consistent with this approach, it is found that (a) the oscillator strength of the donor−acceptor charge transfer (DACT) absorption is roughly proportional to the red shift of ν_{CN} and (b) there are strong symmetry constraints on the coupling. The latter point is demonstrated by a 10-fold larger red shift of the symmetrical than of the antisymmetrical combination of CN^- stretching frequencies in the centrosymmetric *trans*-([14]aneN$_4$)Cr(CNRu(NH$_3$)$_5$)$_2$$^{5+}$ complex ([14]aneN$_4$ = 1,4,7,11-tetraazacyclotetradecane). The coupling of the metal dπ orbitals to CN^- π and π^* orbitals can be formulated in terms of ligand-to-metal (LMCT) and metal-to-ligand (MCLT) charge transfer perturbations. The associated charge delocalizations provide a basis for the synergistic weakening of the C−N bond and D/A coupling.

Introduction

The evaluation of the electronic coupling between electron transfer donors (D) and acceptors (A) has been of continuing fundamental concern in many areas of chemistry.[1−6] When this coupling is sufficiently strong, it can alter several properties of D/A complexes, or, conversely, changes in certain physical and chemical properties of D/A complexes can be used to evaluate the magnitude of the D/A coupling. Thus, the D/A coupling can (a) give rise to a charge transfer (CT) absorption band whose oscillator strength is a function of the coupling;[1−6] (b) result in significant thermodynamic stabilization (ϵ_s^{th}) of the electron transfer ground state (designated D, Ψ_D);[2] and/or (c) influence the rates of D/A electron transfer processes.[1,4−6] In this paper, we describe our experimental observations that when D and A are covalently linked and strongly coupled some internal physical properties of the linker (or bridging ligand) can also reflect the magnitude of D/A coupling. We employ a simple vibronic model to demonstrate how this behavior can arise in adiabatic systems.

In most studies of electron transfer systems, the evaluations of D/A coupling are accomplished by using the crude Born−Oppenheimer approximation (CBOA)[7,8] and first-order perturbation theory arguments.[1] In these approaches, D/A coupling is usually evaluated in terms of the matrix element, $H_{DA} = \langle\Phi_D°|H'|\Phi_A°\rangle$ [H' is the perturbation hamiltonian and the Φ_i's are the diabatic electronic wave functions for the ground ($i = $ D) and excited ($i = $ A) electron transfer states]. For the strongly coupled systems considered here, it is probably more consistent to formulate the D/A coupling in terms of $\beta_{DA} = H_{DA} - SE_D°$, where S is the overlap integral and $E_D°$ is the energy of the diabatic ground state. Equation 1[1,2,6,9] can then be used to evaluate β_{DA}:

$$\beta_{DA} \cong (0.0205/r_{DA})[\epsilon_{max}\Delta\nu_{1/2}\nu_{max}]^{1/2} \qquad (1)$$

in which ϵ_{max}, $\Delta\nu_{1/2}$, and ν_{max} are the maximum absorptivity, the full width at half-height, and the frequency of the DACT absorption band at its absorption maximum, respectively. r_{DA} is the distance between the centers of D and A, and the DACT band shape is assumed to be Gaussian. Since $\beta_{DA}/E_{DA}°$ ($E_{DA}° = E_A° - E_D°$) is the coefficient for mixing excited state character into the ground state, $\Phi_D \cong [\Phi_D° + (\beta_{DA}/E_{DA}°)\Phi_A°]/(1 + \beta_{DA}^2/E_{DA}°^2)^{1/2}$, the amount of ground state stabilization resulting from this mixing, ϵ_s, is given by eq 2 (this is illustrated

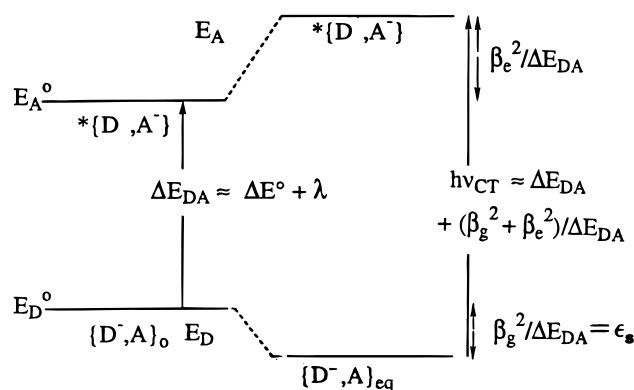$$\epsilon_s \cong \beta_{DA}^2/E_{DA}° \qquad (2)$$

qualitatively in Figure 1). When ϵ_s is sufficiently large, the potential for electrochemical oxidation of D (or reduction of

⊗ Abstract published in *Advance ACS Abstracts,* May 15, 1996.
(1) Newton, M. D. *Chem. Rev.* **1991**, *91*, 767.
(2) Mulliken, R. S.; Person, W. B. *Molecular Complexes*; Wiley Interscience: New York, 1967.
(3) Richardson, D. E.; Taube, H. *Coord. Chem. Rev.* **1984**, *60*, 107.
(4) Creutz, C. *Prog. Inorg. Chem.* **1983**, *30*, 1.
(5) Haim, A. *Comments Inorg. Chem.* **1984**, *4*, 113.
(6) (a) Hush, N. S. *Electrochim. Acta* **1968**, *13*, 1005. (b) *Prog. Inorg. Chem.* **1967**, *9*, 391.
(7) In the sense that the usual electron transfer models[8] assume that the electron jumps between reactant and product configurations only after the nuclei have rearranged.

(8) (a) Marcus, R. A. *Annu. Rev. Phys. Chem.* **1964**, *15*, 155. (b) Marcus, R. A. *Discuss. Faraday Soc.* **1960**, *29*, 21.
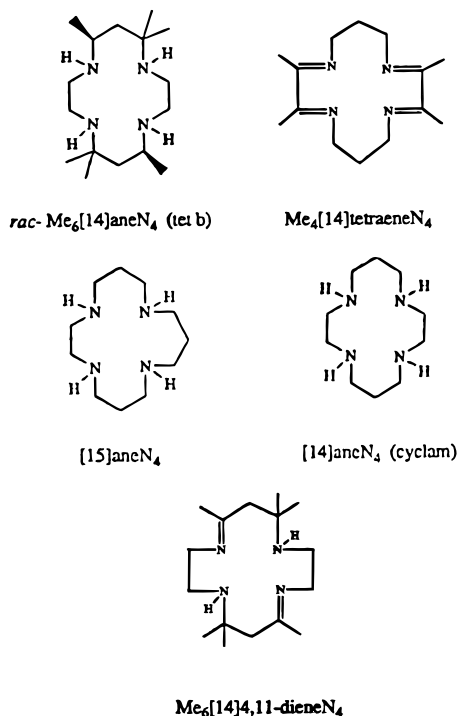(9) Creutz, C.; Newton, M. D.; Sutin, N. *J. Photochem. Photobiol. A: Chem.* **1994**, *82*, 47.

Figure 1. Schematic relationship between the energies of $(E_{DA}°, E_D°)$ of the uncoupled, adiabatic states and the energies of the donor–acceptor ground (g) and excited (e) states after D/A electronic perturbational mixing. Based on ref 2.

A) will reflect contributions from ϵ_s, as in eq 3,[10] where the plus sign is used when D is oxidized (D/D$^+$ redox couple) and

$$E_{1/2}^{obsd} = E_{1/2}^{ref} \pm \epsilon_s^{th} \tag{3}$$

the minus sign when A is reduced (A/A$^-$ redox couple), and $E_{1/2}^{ref}$ is the potential for the redox couple in the absence of DACT coupling. We have used the superscript th to distinguish the stabilization energy, ϵ_s^{th}, inferred from thermodynamic measurements from the value, ϵ_s^{op}, which is inferred from spectroscopic measurements by means of eqs 1 and 2. A puzzle that has evolved in several laboratories' attempts to systematically compare ϵ_s^{th} to ϵ_s^{op} is that ϵ_s^{th} is consistently much larger than ϵ_s^{op};[10-13] for the CN$^-$-bridged complexes considered in this paper, $2 \le (\epsilon_s^{th}/\epsilon_s^{op}) \le 5$.[13] It seemed likely to us that this unexpectedly large value of ϵ_s^{th} in the CN$^-$-bridged complexes might somehow be related to the observation of faster than predicted[14] back electron transfer rates of some photoexcited D(CN$^-$)A complexes (sometimes even faster than vibrational relaxation rates)[15,16] and also that all of these factors must somehow be related to an unusual[17] red shift of the CN$^-$-stretching frequency which usually occurs when CN$^-$ bridges a donor to an acceptor.[10,18] We have now prepared several series of simple CN$^-$-bridged D/A complexes and find that the red shifts of ν_{CN} are roughly correlated with the oscillator strength

(10) (a) Endicott, J. F.; Song, X.; Watzky, M. A.; Buranda, T., Lei, Y. *Chem. Phys.* **1993**, *176*, 427. (b) Endicott, J. F.; Song, X.; Watzky, M. A.; Buranda, T. *J. Photochem. Photobiol. A: Chem.* **1994**, *82*, 181.
(11) (a) de la Rosa, R.; Chang, P. J.; Salaymeth, F.; Curtis, J. C. *Inorg. Chem.* **1985**, *24*, 4229. (b) Salaymeth, F.; Berhaue, S.; Yusof, R.; de la Rosa, R.; Fung, E. Y.; Matamoros, R.; Law, K. W.; Zheng, Q.; Kober, E. M.; Curtis, J. C. *Inorg. Chem.* **1993**, *32*, 3895.
(12) (a) Mines, G. A.; Roberts, J. A.; Hupp, J. T. *Inorg. Chem.* **1992**, *31*, 125. (b) Mines, G. A.; Roberts, J. A.; Bebel, J. C.; Absi, M. P.; Hupp, J. T. *J. Am. Chem. Soc.* **1992**, *114*, 7957.
(13) (a) Watzky, M. A., Ph.D. Dissertation, Wayne State University, Detroit, MI, 1994. (b) Watzky, M. A.; Endicott, J. F.; Buranda, T.; Song, X. *J. Phys. Chem.*, to be submitted.
(14) Buranda, T.; Lei, Y.; Endicott, J. F. *J. Am. Chem. Soc.* **1992**, *114*, 6917.
(15) (a) Doorn, S. K.; Stoutland, P. O.; Dyer, R. B.; Woodruff, W. H. *J. Am. Chem. Soc.* **1992**, *114*, 3133. (b) Doorn, S. K.; Dyer, R. B.; Stoutland, P. O.; Woodruff, W. H. *J. Am. Chem. Soc.* **1993**, *115*, 6398.
(16) (a) Walker, G. L.; Barbara, D. F.; Doorn, S. K.; Hupp, J. T. *J. Phys. Chem.* **1991**, *95*, 5712. (b) Tominaga, K.; Kliner,. D. A. V.; Johnson, A. E.; Levinger, N. E.; Barbara, P. F. *J. Phys. Chem.* **1993**, *97*, 1228. (c) Reid, P. J.; Silva, C.; Barbara, P. F.; Karki, L.; Hupp, J. T. *J. Phys. Chem.* **1995**, *99*, 2609.
(17) Nakamoto, K. *Infrared and Raman Spectra of Inorganic and Coordination Compounds*, 4th ed.; Wiley: New York, 1986.
(18) Bignozzi, C. A.; Argazzi, R.; Schoonover, J. R.; Dyer, R. B.; Scandola, F. *Inorg. Chem.* **1992**, *31*, 5260.

Figure 2. Skeletal diagrams of the macrocylic ligands used in this study. Abbreviations are given in ref 23.

of the DACT absorption band. These observations and the origin of the effect are the focus of the present report.

Experimental Section

Literature procedures were used for the synthesis of (a) [M(bpy)$_2$(CN)$_2$]X complexes with M = Cr,[19] Rh,[20] Fe,[21] and Co[22] ; (b) [M(phen$_2$)(CN)$_2$]X complexes of Rh[20] and Fe[21]; and (c) *cis*- and *trans*-[M(MCL)(CN)$_2$]X complexes in which (MCL) is a tetraazamacrocyclic ligand[23] and M = Cr,[24,25] Rh,[26] and Co.[10a,27] The synthesis of mono- and/or bis(cyanoruthenates) [Ru(NH$_3$)$_5$$^{2+}$ and/or Ru(NH$_3$)$_5$$^{3+}$] have been reported previously for (a) Ru(bpy)$_2$(CN)$_2$;[28] (b) Rh(bpy)$_2$(CN)$_2$$^+$[10a] and Rh(phen)$_2(CN)_2$$^+$;[27] (c) Fe(bpy)$_2(CN)_2$[27] and Fe(phen)$_2(CN)_2$;[27] (d) Co-(bpy)$_2(CN)_2$$^+$;[27] (e) Cr(bpy)$_2(CN)_2$$^+$;[27] (f) *trans*-Co(MCL)(CN)$_2$$^+$ for MCL = [14]aneN$_4$,[10a] *rac*-Me$_6$[14]aneN$_4$,[10a] and Me$_4$[14]tetraeneN$_4$;[27] and (g) [Ru(tpy)(bpy)Cl]Cl.[29] The macrocyclic ligands employed are illustrated in Figure 2.

The [Ru(NH$_3$)$_5$Cl]Cl$_2$ was purchased from Strem Chemical. Research or spectroscopic grade chemicals were used throughout.

(19) Ryu, C. K.; Endicott, J. F. *Inorg. Chem.* **1988**, *27*, 2203.
(20) Gidney, P. M.; Gillard, R. D.; Heaton, B. T. *J. Chem. Soc., Dalton Trans.* **1972**, *23*, 2621.
(21) Schiltt, A. A. *J. Am. Chem. Soc.* **1960**, *82*, 3000.
(22) Maki, N.; Sakuraba, S. *Bull. Chem. Soc. Jpn.* **1969**, *42*, 1908.
(23) Abbreviations of ligand names: Me$_4$[14]tetraeneN$_4$ = 2,3,9,20-tetramethyl-1,4,8,11-tetraazacyclotetradeca-1,3,8,10-tetraene; Me$_6$-[14]4,11,-dieneN$_4$ = 5,7,7,12,14,14-hexamethyl-1,4,8,11-tetraazacy-clotetradeca-4,11-diene; [14]aneN$_4$ = 1,4,8,11-tetraazacyclotetradecane; [15]aneN$_4$ = 1,4,8,12-tetraazaccylopentadecane; *rac*-Me$_6$[14]aneN$_4$ = 5,12-*rac*-5,7,7,12,14,14-hexamethyl-1,4,8,11-tetraazacyclotetradecane.
(24) Kane-Maguire, N. A. P.; Wallace, K. C.; Trzaperk, T. S. *Inorg. Chim. Acta* **1983**, *76*, L179.
(25) Lessard, R. B.; Heeg, M. J.; Buranda, T.; Perkovic, M. W.; Schwarz, C. L.; Rudong, Y.; Endicott, J. F. *Inorg. Chem.* **1992**, *31*, 3091.
(26) Kane-Maguire, N. A. P.; Crippen, W. S.; Miller, P. K. *Inorg. Chem.* **1983**, *22*, 696.
(27) Watzky, M. A.; Song, X.; Endicott, J. F. *Inorg. Chim. Acta.* **1994**, *226*, 109.
(28) Bignozzi, C. A.; Roffia, S.; Scandola, F. *J. Am. Chem. Soc.* **1985**, *107*, 1644.
(29) Dwyer, F. P.; Goodwin, H. A.; Gyarfas, E. C. *Austr. J. Chem.* **1963**, *16*, 92.
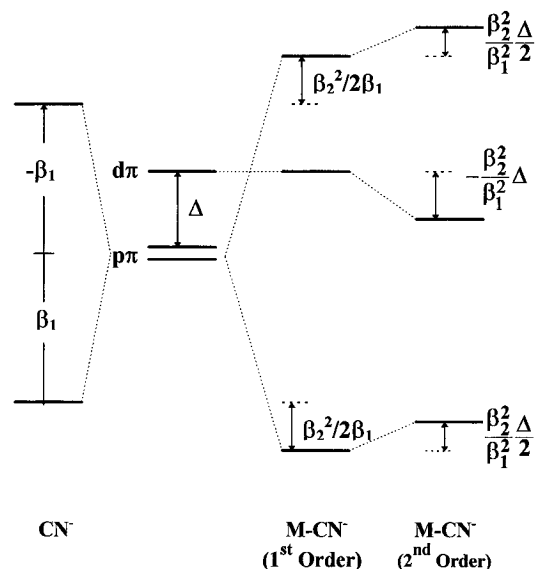
Figure 3. Qualitative illustration of the three-center (see Appendix A) metal−cyanide interactions when there is significant $d\pi/p\pi(C)$ coupling and for $\beta_1 \gg \beta_2$. The figure illustrates the effect of interactions in a single plane (e.g., the $x{-}z$ plane). The left-hand side of the diagram illustrates the expectation for free CN⁻.

In general, we have found that ruthenation of coordinated cyanide was most conveniently accomplished by using $Ru(NH_3)_5OH_2^{2+}$. Aqueous solutions of $Ru(NH_3)_5OH_2^{2+}$ were prepared by the reduction of solutions of $[Ru(NH_3)_5Cl]Cl_2$, purged with Cr^{2+}-scrubbed Ar, using fresh Zn(Hg). The $Ru(NH_3)_5OH_2^{2+}$ solutions were mixed anaerobically with Ar-purged solutions of the $ML(CN)_2^+$ or $M(L)(CN)_2$ complex. All solutions were shielded from light. All reaction mixtures were stirred under Ar for 3−6 h; the ruthenations of $Fe(PP)(CN)_2$ (PP = bpy, phen) complexes could be carried out with Zn(Hg) in the reaction vessel. The reaction products were isolated in an Ar-purged glovebox by precipitation with an excess of NH_4PF_6, and the precipitate was washed with ethanol and ether. Slight variations were made in the general procedure for individual complexes. The complexes metalated with $Ru(NH_3)_5^{3+}$ (M = Ru, Fe) were purified by using a Sephadex SP C-25 resin. The other complexes were purified by repeated washes and recrystallization. Compound purity was determined on the basis of elemental analyses (Table 1), infrared spectra, cyclic voltammetry, and redox titrations. The absorption spectral changes during redox titrations turned out to be especially sensitive to impurities. The purity of a preparation could be assessed by the observation of reasonable isosbestic points and by the stoichiometric changes in absorbance during a redox titration.

The metal ratios in some mixed metal complexes were determined from inductively coupled plasma analyses[30] by using an ICP-EM Optima 3000 apparatus. Samples were referenced to the atomic emission standards of the metals analyzed. This approach gave a Cr/Ru ratio of 1/(1.85 ± 0.05), a Rh/Ru ratio of 1 (1.95 ± 0.05), and a Fe/Ru ratio of 1 (1.95 ± 0.05) for the respective $(bpy)_2M(CNRu(NH_3)_5)_2^{n+}$ complexes. For the complexes with macrocyclic ligands we found the following ratios: (a) Cr/Ru ratios of 1/(1.8 ± 0.2), 1/(0.95 ± 0.10), and 1/(2.0 ± 0.1) for *trans*-Cr([14]aneN₄)(CNRu(NH₃)₅)₂⁵⁺, *cis*-Cr(*rac*-Me₆[14]aneN₄)(CN)(CNRu(NH₃)₅)³⁺, and *cis*-Cr(*rac*-Me₆-[14]aneN₄)(CNRu(NH₃)₅)₂⁵⁺, respectively; (b) Co/Ru ratios of 1/(1.8 ± 0.1) and 1/(1.9 ± 0.1) for *trans*-Co(Me₄[14]tetraeneN₄)(CNRu(NH₃)₅)₂⁵⁺ and *trans*-Co([15]aneN₄)(CNRu(NH₃)₅)₂⁵⁺, respectively.

[(bpy)₂Cr(CN)(CNRu(NH₃)₅)](PF₆)₃. Ar-deareated solutions of $[Ru(NH_3)_5OH_2](CF_3SO_3)_2$ (0.19 g of $[Ru(NH_3)_5O_3SCF_3](CF_3SO_3)_2$, 0.3 mmol)[31] and $[Cr(bpy)_2(CN)_2]CF_3SO_3$ (0.0565 g; 0.1 mmol) in 10 mL of H_2O were mixed under anaerobic conditions. The reaction mixture was stirred at 40 °C under Ar in the dark for 6 h. It was then transferred to an Ar atmosphere glovebox. The blue product was precipitated by

Table 1. Elemental Analyses

	% found (calculated)		
	C	N	H
[Cr(bpy)₂(CN)₂]CF₃SO₃·H₂O	47.44 (47.35)	14.39 (14.40)	2.76 (3.11)
[(bpy)₂Cr(CN)(CNRu(NH₃)₅)](PF₆)₃·2H₂O	24.90 (24.61)	13.94 (14.35)	2.98 (3.29)
[(bpy)₂Cr(CN)(CNRu(NH₃)₅)₂](PF₆)₅	18.08 (17.46)	14.02 (14.81)	3.09 (3.06)
[Rh(bpy)₂(CN)₂]CF₃SO₃·H₂O	43.69 (43.55)	12.97 (13.25)	2.83 (2.86)
[(bpy)₂Rh(CN)(CNRu(NH₃)₅)](PF₆)₃· NH₄PF₆·H₂O	20.77 (20.82)	13.51 (13.24)	2.99 (2.94)
[(bpy)₂Rh(CNRu(NH₃)₅)₂](PF₆)₅	17.93 (16.89)	13.43 (14.32)	2.83 (2.96)
Fe(bpy)₂(CN)₂·H₂O	57.41 (57.91)	18.24 (18.42)	4.49 (4.42)
[*trans*-Co(Me₄[14]tetraeneN₄)(CN)₂]PF₆	37.94 (38.10)	16.40 (16.67)	4.86 (4.80)
[*trans*-Co([15]aneN₄)(CN)₂]PF₆·¹/₃NH₄PF₆	29.86 (29.76)	16.37 (16.91)	5.18 (5.25)
[*trans*-([14]aneN₄)Cr(CNRu(NH₃)₄.₅-(OH₂)₀.₅)₂](PF₆)₅	10.75 (10.28)	14.63 (14.98)	3.74 (3.81)
[*cis*-(rac-Me₆[14]aneN₄)Cr(CNRu-(NH₃)₅)₂](PF₆)₅	14.08 (14.55)	14.51 (15.08)	4.45 (4.48)
[*trans*-(Me₄[14]tetraeneN₄)Co-(CNRu(NH₃)₄.₅ (OH₂)₀.₅)₂](PF₆)₅	13.65 (13.18)	14.11 (14.41)	3.36 (3.67)
[trans-Co([14]aneN₄)(CN)₂]Cl	41.06 (41.57)	23.99 (20.24)	7.02 (6.98)
[*trans*-([14]aneN₄)Co(CNRu(NH₃)₅)₂](PF₆)	10.30 (10.21)	15.55 (15.89)	3.84 (3.86)
[*trans*-(Me₆[14]dieneN₄)Co-(CNRu(NH₃)₅)₂](PF₆)₅	14.60 (14.50)	14.80 (15.09)	4.13 (4.19)
[(bpy)₂Fe(CNRu(NH₃)₄OH₂)₂](PF₆)₄	18.72 (18.98)	14.13 (14.08)	3.33 (3.33)
Fe(phen)₂(CN)₂	66.44 (66.68)	17.93 (17.95)	3.36 (3.44)
[Co(bpy)₂(CN)₂][NO₃]·2H₂O	50.48 (50.68)	18.38 (18.81)	4.60 (3.87)
[Co(phen)₂(CN)₂]NO₃·3.5H₂O	52.34 (52.36)	16.64 (16.44)	4.05 (3.89)
[Ru(tpy)(bpy)CN]ClO₄·0.3NaClO₄	47.23 (47.55)	12.22 (12.80)	2.89 (2.92)
[(tpy)(bpy)Ru(CNRu(NH₃)₃(OH₂)₂)][PF₆]₄	24.21 (24.31)	10.09 (9.81)	3.00 (2.51)
[*cis*-Cr-Me₆(rac-Me₆[14]aneN₄)(CN)₂]-(CF₃SO₃)·2H₂O	40.26 (39.78)	14.69 (14.65)	6.49 (7.03)

adding a minimum amount of NH_4PF_6 to the solution and cooling it down to 0 °C. It was isolated by filtration and washed with cold H_2O, EtOH, and EtO (yield, 55%). The material was then kept in the refrigerator in an Ar-purged vial protected from light.

[(bpy)₂Cr(CNRu(NH₃)₅)₂](PF₆)₅. A blue product was obtained with modification of the preceding procedure: solutions of $[Ru(NH_3)_5OH_2]$-Cl_2 (0.25 mmol) and $[Cr(bpy)_2(CN)_2]Cl$ (0.1 mmol) were concentrated to 5 mL, and the reaction was run at room temperature.

[(bpy)₂Rh(CNRu(NH₃)₅)₂](PF₆)₃. An orange-brown product was obtained by metalation of $[Rh(bpy)_2(CN)_2]CF_3SO_3$ by using the procedure for $[(bpy)_2Cr(CN)(CNRu(NH_3)_5)](PF_6)_3$, except that the reaction was run at room temperature (yield, 80%).

[(bpy)₂Rh(CNRu(NH₃)₅)₂](PF₆)₅. An orange-brown product was obtained by metalation of $[Rh(bpy)_2(CN)_2]Cl$ by using the procedure for $[(bpy)_2Cr(CNRu(NH_3)_5)_2](PF_6)_5$.

[(phen)₂Rh(CNRu(NH₃)₅)₂](PF₆)₅. An orange-brown product was obtained by metalation of $[Rh(phen)_2(CN)_2]Cl$ by using the preceding procedure.

[(bpy)₂Fe(CN)(CNRu(NH₃)₅)](PF6)₅. A purple product was obtained by metalation of $Fe(bpy)_2(CN)_2$ byusing the procedure for $[(bpy)_2Cr(CN)(CNRu(NH_3)_5)](PF_6)_3$ (yield, 45%).

[(bpy)₂Fe(CNRu(NH₃)₅)₂](PF₆)₄. A purple product was obtained by metalation of $Fe(bpy)_2(CN)_2$ by using the procedure for $[(bpy)_2Cr-(CNRu(NH_3)_5)_2](PF_6)_3$, except that the reaction was run on Zn(Hg) (yield, 45%).

[(bpy)₂Fe(CNRu(NH₃)₅)₂]Cl₆. Air oxidation of aqueous solutions of $(bpy)_2Fe(CNRu(NH_3)_5)_2^{4+}$ resulted in unidentified decomposition

(30) Blades, M. W.; Weir, D. G. *Spectroscopy* **1994**, *9*, 14.
(31) Dixon, N. E.; Lawrence, G. A.; Lay, P. A.; Sargeson, A. M.; Taube, H. *Inorg. Synth.* **1986**, *24*, 243.

products. It thus was oxidized chemically and anaerobically to $(bpy)_2Fe(CNRu(NH_3)_5)_2^{4+}$ by the addition of a stoichiometric amount of $Fe(H_2O)_6^{3+}$ [0.1 M $Fe(NO_3)_3$ in 1 M CF_3SO_3H]. It could then be separated on a Sephadex SP-C25−120 cation exchange column in the Na^+ form and eluted with a 1 M NaCl solution. The $Fe(bpy)_2(CN)_2$ and $(bpy)_2Fe(CN)(CNRu(NH_3)_5)^{3+}$ impurities were eluted with 0.25 and 0.5 M NaCl, respectively. A resin in the H^+ form and/or H^+ elution lead to product decomposition. Care was taken to protect solutions from light, and efficient band separation was obtained by making gradients of eluant concentration. Unfortunately, the product could not be separated from the excess NaCl, and materials were used for spectroscopic analysis only.

[(phen)₂Fe(CNRu(NH₃)₅)₂](PF₆)₄. A purple product was obtained by metalation of $Fe(phen)_2(CN)_2$ by using the preceding procedure (yield, 70%).

[*trans*-Cr([14]aneN₄)(CNRu(NH₃)₅)₂](PF₆)₅. A brick-red product was obtained by metalation of [*trans*-Cr([14]aneN₄)(CN)₂]Cl (in suspension in H_2O) by using the procedure for [(bpy)₂Cr(CNRu(NH₃)₅)₂]-(PF₆)₅ (yield, 60%).

[*cis*-Cr(*rac*-Me₆[14]aneN₄)(CN)(CNRu(NH₃)₅)](PF₆)₃. A deep-purple product was obtained by metalation of [*cis*-Cr(*rac*-Me₆[14]aneN₄)(CN)₂]CF₃SO₃ (in suspension in H_2O) by using the procedure for [(bpy)₂Rh(CN)(CNRu(NH₃)₅)](PF₆)₃ (yield, 55%).

[*cis*-Cr(*rac*-Me₆[14]aneN₄)(CNRu(NH₃)₅)₂](PF₆)₅. A deep-purple product was obtained by metalation of [*cis*-Cr(*rac*-Me₆[14]aneN₄)(CN)₂]-Cl (in suspension in H_2O) by using the procedure for [*trans*-([14]aneN₄)-Cr(CNRu(NH₃)₅)₂](PF₆)₅.

[(tpy)(bpy)RuCN]CF₃SO₃. A sample of [(tpy)(bpy)RuCl]Cl was treated with concentrated HO_3SCF_3 to generate [(tpy)(bpy)RuO₃-SCF₃]CF₃SO₃.[28] A 0.18 g sample of this salt (0.23 mmol) was refluxed overnight in 30 mL of MeOH/H_2O (1/1, v/v) containing 0.3 g of KCN (in 20× excess). The solution turned reddish-brown, and methanol was evaporated from the reaction mixture on a steam bath. The product precipitated out of the cooled solution. It was separated by filtration, washed with cold H_2O, and dried with Et_2O (yield, 75%).

[(tpy)(bpy)Ru(CNRu(NH₃)₅)](PF₆)₄. A brown product solution was obtained by metalation of [(tpy)(bpy)RuCN]Cl by using the procedure for $(bpy)_2Fe(CNRu(NH_3)_5)_2^{4+}$, except that the reactants were in a 1/1 molar ratio. The reaction mixture was open to air after the removal of Zn(Hg) (a few drops of H_2O_2 could be added); it turned green overnight. It was then chromatographed on a Sephadex SP C25−120 cation exchange resin (H^+ form), where care was taken to protect the column from light during separations. The green product was eluted with 0.6 M HCl by using gradients of eluant concentration [the Ru(tpy)(bpy)-CN$^+$ impurity was eluted with 0.3 M HCl]. The solvent was removed by rotary evaporation, and the residue was recrystallized in H_2O with NH_4PF_6.

With the notable exception of the $Ru(bpy)_2(CN)_2$ ruthenates, these were not very stable compounds. The $Ru(NH_3)_5^{2+}$ metalates were easily oxidized, and for M = Rh, Co, and Cr solutions, the $Ru(NH_3)_5^{3+}$ metalates showed signs of decomposition within an hour or so. Most complexes had a common impurity/decomposition product that exhibited an intense absorbance at about 900 nm.[32] In the original samples used in this study this species constituted less than 5% of the solid compound on the basis of its redox stoichiometry.

Infrared spectra were obtained by using samples in KBr pellets and a Nicolet 20 DXM FT-IR spectrometer. Procedures for UV−visible spectroscopy, redox titrations, and electrochemistry are described elsewhere.[10,13]

Results

The results of the spectroscopic measurements are summarized in Table 2. One expects to find two CN^- stretching frequencies in the parent $(L)_4M(CN)_2^{n+}$ complexes, i.e., the symmetric and antisymmetric combinations of CN^- stretching frequencies. In centrosymmetric *trans* complexes, only the antisymmetric combination will be fully IR allowed, but both stretching frequencies should be IR active in the *cis* complexes (which have either C_2 or C_{2v} symmetry). The resolution of two CN^- stretching frequencies in the lower symmetry parent complexes will depend on the difference in their energies and, thus, on the extent of metal-mediated coupling of these vibrations. In many of these complexes we resolved only one CN^- stretch in the IR, implying near degeneracy of the symmetry-adapted stretches and consequently weak coupling of the vibrational motions. These splittings were never large (≤ 12 cm^{-1}) in any of the parent *cis* complexes. The intensity of ν_{CN} tended to increase upon ruthenation, two components were more commonly observed, and their frequency differences ($\Delta\nu_{s,a}$) tended to increase. The most dramatic effects were found among the metalates of $Ru(bpy)_2(CN)_2$. It probably is not surprising that the largest value of $\Delta\nu_{s,a}$ (46 cm^{-1}) was found in $(bpy)_2Ru(CNRu(NH_3)_5)_2^{6+}$, in which there is appreciable D/A coupling. That a similar value of $\Delta\nu_{s,a}$ was not resolved for the $(bpy)_2Cr(CNRu(NH_3)_5)_2^{5+}$ analog suggests a dependence of this vibrational coupling on the electronic structure of the central metal. In contrast, $\Delta\nu_{s,a} \cong 45$ cm^{-1} for *trans*-Cr([14]aneN₄)-(CN)₂$^+$, with the antisymmetric combination of CN^- stretches having the lowest frequency.

While the simplest interpretation of these observations probably involves molecular orbital arguments related to those developed in the following, the values of $\Delta\nu_{s,a}$ are not the focus of this report, but they are of concern because they do introduce some uncertainty into the trends in $\Delta\nu_{CN}$ discussed later. This uncertainty arises from the symmetry constraints on the mixing of DACT excited states with the ground state and the expectation that one of the symmetry-adapted components of the CN^- stretches should be much more strongly implicated in D/A coupling than the other. Unfortunately, the symmetry-adapted combinations are not easily identified in the low-symmetry complexes. When $\Delta\nu_{s,a}$ is small, we use an average of the observed frequencies in evaluating $\Delta\nu_{CN}$. In the ruthenated complexes with large values of $\Delta\nu_{s,a}$, we based our values of $\Delta\nu_{CN}$ on a comparison of mono- and diruthenated complexes. In the centrosymmetric complexes, the more intense of the CN^- stretches can be confidently assigned as the antisymmetric combination, and we have inlcuded some preliminary details of the *trans*-([14]aneN₄)Cr(CNRu(NH₃)₅)₂$^{5+}$ and *trans*-Cr([14]-aneN₄)(CN)₂$^+$ complexes, for which we have resolved ν_s and ν_a. Work in progress on these and related systems[33] may resolve some of the issues regarding $\Delta\nu_{s,a}$.

It is clear from Table 2 that ν_{CN} in the parent complexes strongly depends on the central metals. On the whole these values seem to depend more on the central metal than on the coordinated ligands. However, important symmetry issues are involved, as is illustrated by our preliminary observations on the *trans*-Cr([14]aneN₄)(CN)₂$^+$ complex and its ruthenate. The purpose of the present report is to map out the overall patterns associated with CN^--mediated D/A coupling. Details such as symmetry constraints ultimately will be important in interpreting these patterns, but they are not the major issue at the present time.

To facilitate the comparisons developed in the following section, DACT spectroscopic data from several sources have been incorporated into Table 2. Details of the spectroscopic studies have been published[7,28] or can be found elsewhere.[13]

Discussion

The work presented here is a part of our systematic studies of cyanide-bridged, donor−acceptor complexes. In the very

---

(32) We have prepared a $[Ru(NH_3)_5]_2CN^{4+}$ species for which the molar absorptivity is 4.2×10^3 M^{-1} cm^{-1} for a broad ($\Delta\nu_{1/2} = 5.6 \times 10^3$ cm^{-1}) absorption at 890 nm.[13a]

(33) Macatangay, A.; Watzky, M. A.; Mazzetto, S. E.; Endicott, J. F. Work in progress.

Table 2. Comparison of Cyanide Stretching Frequencies and DACT Spectroscopic Parameters in Cyanometalates and Parent $(L_4)M(CN)_2$ Complexes

complex[a]	ν_{CN} (cm^{-1})[b]	$\lambda_{max}(\epsilon_{max}/10^3)$ $[\Delta\nu_{1/2}/10^3]$[c]	$\Delta\nu_{CN}$ (cm^{-1}) (red shift)[d]	β_{DA} (cm^{-1})[e] (per Ru)	$\epsilon_s{}^{op}$ (cm^{-1})[f]	$E_{DA}{}^{\circ}$ [g] (cm$^{-1}/10^3$)
		DACT parameters				
Cr(III) Centers and Their Ru(NH₃)₅²⁺ Cyanometalates						
$Cr(bpy)_2(CN)_2{}^+$	2134 (w)					
$(bpy)_2Cr(CN)(CNRu(NH_3)_5)^{3+}$	2071, 2107 (sh)	645 (3.60) [6.05]	63	2290	380	13.3
$(bpy)_2Cr(CNRu(NH_3)_5)_2{}^{5+}$	2073	655 (6.0) [5.65]	61	2005	290	13.5
trans-$Cr(L_1)(CN)_2{}^+$	2093 (w), a 2139 (w), s					
trans-$Cr(L_1)(CNRu(NH_3)_5)_2{}^{5+}$	2074, a 1997, s	500 (8.00) [4.90]	14	2470	340	18.0
cis-$Cr(L_3)(CN)_2{}^+$	2132 (w)					
cis-$Cr(L_3)(CN)(CNRu(NH_3)_5)^{3+}$	2077	530 (3.20) [5.00]	55	2170	270	17.3
cis-$Cr(L_3)(CNRu(NH_3)_5)_2{}^{5+}$	2070	522 (8.00) [5.10]	62	2465	350	12.1
Ru(II) Centers and Their M(NH₃)₅³⁺ Cyanometalates (M = Ru or Rh)						
$Ru(bpy)_2(CN)_2$	2060, 2072 (s)					
$(bpy)_2Ru(CN)(CNRu(NH_3)_5)^{3+}$	2019, 2075	700 (4.45) [4.50]	41	2110	365	12.2
$(bpy)_2Ru(CNRu(NH_3)_5)_2{}^{6+}$	2011, 2057	655 (7.77) [5.00]	49, 15	2145	346	13.3
$(bpy)_2Ru(CNRh(NH_3)_5)(CNRuNH_3)_5)_2{}^{6+}$	2019, 2121	670 (~5.4)[h] [5.28]	41, −49	~2 × 10³		
$(bpy)_2Ru(CN)(CNRh(NH_3)_5)^{3+}$	2062, 2105[i]		−33			
$(bpy)_2Ru(CNRh(NH_3)_5)_2{}^{6+}$	2105, 2124[i]		−45, −52			
$Ru(tpy)(bpy)CN^+$	2076(5)					
$(tpy)(bpy)Ru(CNRu(NH_3)_5)^{4+}$	2020	700 (4.10) [4.90]	56	2110	365	12.1
Ru(II) Center with Ru(NH₃)₅²⁺ Cyanometalate						
$(bpy)_2Ru(CNRu(NH_3)_5)_2{}^{4+}$	2090, 2130[j,k]		−30, −58			
Fe(II) Centers and Their Ru(NH₃)₅³⁺ Cyanometalates						
$Fe(bpy)_2(CN)_2$	2070, 2078 (s)					
$(bpy)_2Fe(CNRu(NH_3)_5)_2{}^{6+}$	2033, 2019	875 (6.58) [4.75]	58, 37	1670	290	9.7
$Fe(phen)_2(CN)_2$	2065, 2079 (s)					
$(phen)_2Fe(CNRu(NH_3)_5)_2{}^{6+}$	~2025	880 (6.80) [4.75]	47	1690	300	9.6
Fe(II) Centers with Ru(NH₃)₅²⁺ Cyanometalates						
$(bpy)_2Fe(CNRu(NH_3)_5)_2{}^{4+}$	2091, 2081		−13, −11			
$(phen)_2Fe(CNRu(NH_3)_5)_2{}^{4+}$	~2080					
Co(III) Centers and Their Ru(NH₃)₅²⁺ Cyanometalates						
$Co(bpy)_2(CN)_2{}^+$	2142					
$Co(bpy)_2(CN)_{2-n}(CNRu(NH_3)_5)_n{}^{(2n+1)+}$	2134[o]	415 (0.60) [13.403][m,p]	8	1230	64	23.7
trans-$Co(L_4)(CN)_2{}^+$	2135					
trans-$Co(L_4)(CNRu(NH_3)_5)_2{}^{5+}$	2125	520 (1.80) [6.60]	10	1370	100	18.6
trans-$Co(L_6)(CN)_2{}^+$	2130					
trans-$Co(L_6)(CNRu(NH_3)_5)_2{}^{5+}$	2108	518 (0.64) [6.00]	22	760	30	19.1
trans-$Co(L_1)(CN)_2{}^+$	2130					
trans-$Co(L_1)(CNRu(NH_3)_5)_2{}^{5+}$	2110	501 (1.03) [7.01]	20	1060	57	19.6
trans-$Co(L_5)(CN)_2{}^+$	2125					
trans-$Co(L_5)(CNRu(NH_3)_5)_2{}^{5+}$	2111	511 (1.03) [7]	14	1060	58	19.2
Rh(III) Centers and Their Ru(NH₃)₅²⁺ Cyanometalates						
$Rh(bpy)_2(CN)_2{}^+$	2141, 2148 (s)					
$(bpy)_2Rh(CN)(CNRu(NH_3)_5)^{3+}$	2143	j,l	1 (av)		~0[j]	
$(bpy)_2Rh(CNRu(NH_3)_5)_2{}^{5+}$	2140	j,l	4 (av)		~0[j]	
$Rh(phen)_2(CN)_2{}^+$	2144					
$(phen)_2Rh(CNRu(NH_3)_5)_2{}^{5+}$	2140		4 (av)		~0[h]	
trans-$Rh(L_1)(CN)_2{}^+$	2126					
trans-$Rh(L_1)(CNRu(NH_3)_5)_2{}^{5+}$	2110	m,n	16		~0	

 ^{a} Macrocyclic ligands:[23] L_1 = [14]aneN₄ (cyclam); L_2 = *rac*-Me₆[14]aneN₄; L_3 = Me₄[14]tetraeneN₄; L_4 = [15]aneN₄; L_5 = Me₆[14]dieneN₄. ^{b} w, weak; s, strong; vw, very weak; no designation implies medium; sh, shoulder. For *trans*-$CrL_1(CN)_2$ complexes, a indicates an antisymmetric and s a symmetric combination of CN⁻ stretches. ^{c} Wavelength in nanometers, molar absorptivity in cm^{-1} M^{-1}, and full width at half-maximum intensity in cm^{-1}. Parameters are from refs 10, 13, and 27. ^{d} Cyanide stretch of parent complex minus that of the metalate. ^{e} β_{DA} calculated from eq 1. ^{f} $\epsilon_s{}^{op}$ = $(\beta_{DA}{}^{\circ})^2/E_{DA}{}^{\circ}$. ^{g} Based on $E_{DA}{}^{\circ} \cong E_{op} - 2\epsilon_s{}^{th}$ and $\epsilon_s{}^{th} \cong 3\epsilon_s{}^{op}$.[13] ^{h} By weight of salt; absorption in acetonitrile. All others are from redox titrations in water. ^{i} References 14 and 34. ^{j} Lowest energy transition is assigned as Ru(NH₃)₅²⁺ → bpy (or phen) CT. No DACT absorption is observed (see refs 27 and 28). ^{k} Reference 18. ^{l} Reference 27. ^{m} Refseferences 10 and 13. ^{n} Lowest energy transition is assigned as Ru(NH₃)₅²⁺ → CN⁻(π^*). ^{o} Reference 27. This complex is most likely a monoruthenate ($n = 1$). ^{p} The DACT and Ru(NH₃)₅²⁺ → bpy CT absorptions are convoluted; ϵ_{max} per Ru.

early stages of this work,[34] we observed that the CN⁻ stretches were appreciably red shifted in D(CN⁻)-A complexes, and this red shift has proved to be a very useful guide to the successful synthesis of CN⁻-bridged D/A complexes. The present report represents our efforts to determine the reason for the shift of

ν_{CN} to lower energy in D/A complexes, in such marked contrast to expectation.[17] While this work was in progress, Bignozzi *et al.*[18] presented a report of their studies of ν_{CN} in CN⁻-bridged d⁶ and d⁵ metal complexes. These workers attributed the observed shifts in ν_{CN} to a combination of dπ/π^*(CN⁻) back-bonding and the kinematic effect discussed by Nakamoto.[17] Our observations, summarized in Table 2, are consistent with those

(34) Lei, Y. Ph.D. Dissertation, Wayne State University, Detroit, MI, 1989.

of Bignozzi *et al.*[18] However, their interpretation in terms of two opposing effects plus an enhancement of back-bonding in the presence of an acceptor is too vague to be useful since the origin of the enhancement is not clear, and since it does not readily account for the symmetry dependent shifts that we have observed. We develop a more rigorous and general interpretation here. First we consider the parent complexes and μ-cyano complexes that do not contain D/A pairs. In these complexes, simple models involving opposing effects work reasonably well. The studies of CN^--bridged D/A complexes demonstrate that these two effects cannot account for the red shift of ν_{CN} in $D(CN^-)A$ complexes. It also appears that even in the absence of bridged donors and acceptors the variations in ν_{CN} are complicated. Nevertheless, these shifts in ν_{CN} can be regarded as sensitive indices of the shifts of electron density across the $M(CN^-)M'$ coordinate. Some approaches to interpreting the shifts of ν_{CN} follow.

A. Some Patterns in the Shifts of ν_{CN}. 1. The Parent Complexes. These parent complexes exhibit a very consistent pattern: (a) for the Rh(III), Co(III), and (Cr(III) (C_2 or C_{2v} symmetry) complexes $(\nu_{CN})_{av} \cong 2134$ cm^{-1}, (b) while for Fe(II) and Ru(II) complexes $(\nu_{CN})_{av} = 2074$ and 2066 cm^{-1}, respectively. The shifts in ν_{CN} for monometal complexes are to lower energy for the more ionizable metals, which is consistent with the hypothesis that $d\pi/\pi^*(CN^-)$ back-bonding is important as an origin of these shifts.[35] An important exception to the value of $\nu_{CN} \cong 2134$ cm^{-1} for M(III)-centered complexes occurs for the centrosymmetric *trans*-Cr([14]aneN$_4$)-$(CN)_2^+$. Two CN^- stretching frequencies have been resolved for this complex: the more intense of these very weak absorptions is at 2094 cm^{-1} and is attributable to ν_a, while a higher energy absorption (2135 cm^{-1}) of about 25% of the intensity of ν_a can be attributed to ν_s. It is important to observe that ν_a for this complex is comparable to $(\nu_{CN})_{av}$ for the Ru(II)- and Fe(II)-centered complexes, and this clearly demonstrates that $d\pi/\pi^*(CN^-)$ back-bonding or electrostatic polarization is not sufficient to account for the lower energy values of ν_{CN} in the monometal complexes. Nevertheless, for our purposes it is sufficent to use a simple, Hückel-type, three-center molecular

orbital model for the π interactions.[37,38] Thus, we attribute the larger variations in ν_{CN} to the following: (a) factors (partly electrostatic) that affect the distribution of electron density within the CN^- moiety (possibly increasing ν_{CN} by about 15 cm^{-1} per unit increase in *formal* charge on M);[35] (b) delocalization of charge from M(II) to CN^- (back-bonding) or from CN^- to M(III), both of which tend to weaken the CN^- bond (see Appendix A) and result in a red shift; and (c) some repulsive coupling between electrons of the bridged metals and those of CN^-.[39] Electrostatic polarization effects that might be postulated[35] to complicate the comparison of Rh(III), Cr(III), and Co(III) complexes on the one hand to Fe(II) and Ru(II) complexes on the other can be referenced against [Pt(tpy)CN]-CF_3SO_3 or Pt(bpy)(CN)$_2$ [$\nu_{CN} = 2141$, 2130, and 2120 cm^{-1}, respectively,[40] which are comparable to values found in the M(III) complexes employed here]. The charge delocalizations between M and CN^- can be viewed conveniently as partial bonding interactions; in the limit of full bond formation, one would have to consider structures such as $M=C=N^-$ analogous to those postulated for metals bridged by polyynes.[41,42]

2. Complexes with Bridging CN^-. The most striking of the observations on μ-cyano complxes are as follows: (a) that bridging of two easily ionizable metals, $M^{II}-(CN^-)-Ru^{II}$ (M = Ru or Fe), results in a blue shift of ν_{CN}, while (b) bridging of a D/A pair, $M^{II}-(CN^-)-Ru^{III}$ (M = Fe or Ru) or $Cr^{III}-(CN^-)-Ru^{II}$, results in a red shift. The first of these observations is superficially surprising because one might expect twice as much back-bonding as observed in the $M^{II}(CN^-)$ parents; however, these observations on the $M^{II}(CN^-)Ru^{II}$ complexes are consistent with the ideas sketched earlier. On the other hand, the shifts of ν_{CN} for the bridged D/A pairs are not consistent with those ideas, and they implicate a vibronic approach to bridging ligand-mediated D/A coupling.

a. Shifts in ν_{CN} for Bridged Complexes without D/A Coupling. We first note that, in complexes of the types $Ru^{II}-(CN^-)-Rh^{III}$ and $Rh^{III}-(CN^-)-Ru^{II}$, ν_{CN} occurs at relatively high energies ($2105-2140$ cm^{-1}), i.e., higher than or equal to those of the parent dicyano complex. We also observe that ν_{CN} is roughly comparable for the $Ru^{II}-(CN^-)-Ru^{II}$ and $Fe^{II}-(CN^-)-Ru^{II}$ complexes (these comparisons are somewhat complicated by the relatively large values of $\Delta\nu_{s,a}$ for these

(35) Some caution should be exercised in developing these simple comparisons since large variations in ν_{CN} are observed when back-bonding is not an issue; e.g., values of 2049 for crystalline KCN[17] and 2273 for gaseous HCN[36] have been reported. A reviewer has also pointed out that electrostatic polarization (internal Stark effect) can contribute to variations in ν_{CN}[35c] and that there is some variation in charge among the complexes considered here. It is concern for these and related issues that has led us to consider a large number of complexes in Table 2. Some of these complexes were synthesized to evaluate the charge issue experimentally, since evaluation of the actual charge at a metal center is very difficult. A simple molecular orbital argument is developed here largely for consistency with our interpretation of the behavior of μ-cyano systems. This is certainly an oversimplification, but, as noted in the text, this approach does provide a more facile interpretation of the observations than does a purely electrostatic approach. We should also note that in the present series of compounds we have found shifts of as much as 10 cm^{-1} in ν_{CN} in different salts of the same complex (larger among the parent complexes than the metalates) and that oxidation of Ru(NH$_3$)$_5^{2+}$ in some of the Co(III)(MCL)(CNRu(NH$_3$)$_5$)$_2^{5+}$ complexes resultes in materials with $\nu_{CN} \cong 2150$ cm^{-1}. While these oxidation products are unstable and difficult to fully characterize, the blue shift of about 15 cm^{-1} that accompanies oxidation might well be taken as a measure of the effect of one unit change in charge. A small increase in ν_{CN} with electric field intensity seems consistent with other experimental observations. (a) Stuhlman, C.; Villegas, I.; Weaver, M. J. *Chem. Phys. Lett.* **1994**, *219*, 319. (b) Spitzer, R. C.; Sievers, A. J.; Silsbee, R. H. *J. Opt. Soc. Am. B* **1992**, *9*, 978. A theoretical treatment of the purely electrostatic (internal Stark) effect on ν_{CN} has been presented: (c) Reimers, J. R.; Zeng, J.; Hush, N. S. *J. Phys. Chem.* **1996**, *100*, 1498.

(36) Herzberg, G. *Infrared and Raman Spectra of Polyatomic Molecules*; Van Nostrand: Princeton, NJ, 1945.

(37) The model developed in Appendix A presumes low symmetry. By restricting consideration to a plane for the centrosymmetric complexes mentioned here, the axial $\pi/d\pi/\pi$ three-center interaction can be approximately treated in a Hückel approach as giving rise to bonding (g), antibonding (g) and nonbonding (u) molecular orbitals. From this perspective, the LMCT excited state would be antisymmetric (u), and mixing with the ground state would have to be promoted by an antisymmetric vibration. This would qualitatively account for the observation that $\nu_a < \nu_s$ in the Cr(III) parent complex. Since the $d\pi$ oribtials are fully occupied in Co(III) and Rh(III), only mixing with MLCT $d\pi/\pi^*(CN^-)$ excited states would be relevant, and these occur at relatively high energies with small mixing coefficients. Hence, $\Delta\nu_{s,a}$ is probably smaller for the centrosymmetric Co(III) and Rh(III) complexes than for the Cr(III) complexes. Symmetry issues in these systems are actually quite complicated, and they will be discussed in detail elsewhere.[13,33] Furthermore, one expects that the differences in the effective reduced masses will generally lead to $\nu_a < \nu_s$ in all of the complexes, even when other effects are not important.

(38) Cotton, F. A. *Chemical Applications of Group Theory*, 3rd ed.; Wiley: New York, 1990; pp 180–188.

(39) This repulsion could, in principle, include electrostatic as well as inertial effects.[14] However, we have not found significant variations in ν_{CN} that can be easily attributed to different masses of the coordinated metals. We simply treat this effect as interelectronic repulsion in the MO argument.

(40) Waknine, D. Ph.D. Dissertation, Wayne State University, Detroit, MI, 1994.

(41) Zhou, Y.; Seyler, J. W.; Weng, W.; Arif, A. M.; Gladysz, J. A. *J. Am. Chem. Soc.* **1993**, *115*, 8509.

(42) Lapinte, C.; Toupet, L.; Le Narvor, N. *J. Am. Chem. Soc.* **1995**, *117*, 7129.
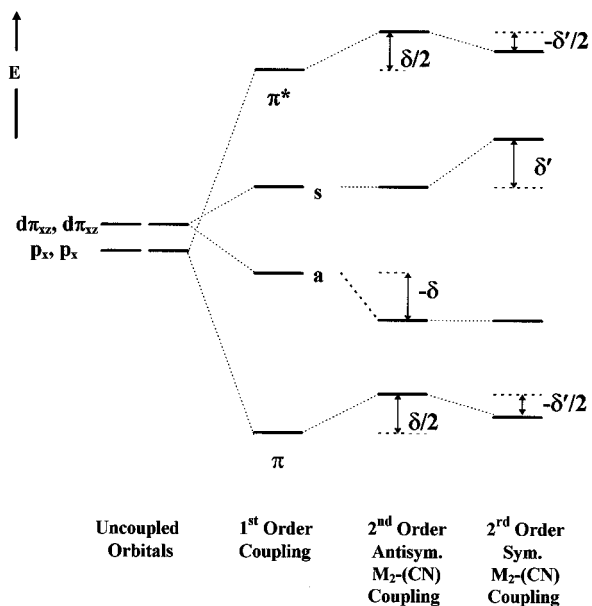
Figure 4. Qualitative illustration of metal−cyanide interactions when CN$^-$ bridges two metals for which back-bonding, dπ/π*, interactions are significant. The pattern of orbital energies has been generated in terms of the superposition of two symmetry-adapted three-center interactions; in the centrosymmetric limit, these three-center interactions would correspond to the symmetric and antisymmetric combinations of atomic orbitals, assuming that the coupling within the bridging ligand (β_1 for CN$^-$) is much larger than that (β_2) between the bridging ligand and the terminal metals. It is assumed that the bridged metals do not form a donor−acceptor pair. The "second-order" perturbation terms, δ and δ', may be different in the M−(CN$^-$)−M′ complexes since the coupling and orbital energy terms (β_2 and Δ for M/C and β' and Δ' for N/M′) may be different.

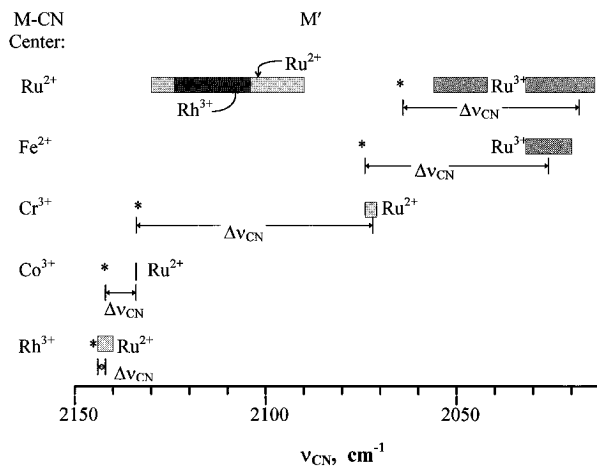complexes). From a molecular orbital point of view, the latter observation is qualitatively reasonable since the back-bonding contributions at opposing ends of the CN$^-$ bridge would have to involve out-of-phase orbital contributions, and thus they would be repulsive. This is readily accommodated in an extension of the arguments in the preceding section: (a) the antisymmetric combination of dπ_a and dπ_b will only mix with the π* ligand orbital; and (b) the symmetric combinations will only mix with the π ligand orbital. The net result will be stabilization of the bridging ligand's π orbitals [i.e., in the symmetrical limit $E(\pi) \cong E°(\pi) - \delta/2$, where δ is a perturbational correction term; (see Appendix A); since these are not symmetrical systems, one expects some relaxation of these symmetry constraints]. Thus, the symmetry-adapted MO argument suggests that there is a contrast in the behavior of monometal and bridged "back bonding" bimetallic complexes because there is a competition between "attractive" and "repulsive" interactions[43] in the bridged complexes, leading to a partial cancellation of the second order components of the multicenter perturbation, and this results in a smaller amount of charge delocalized in the bimetallic complexes. This is illustrated qualitatively in Figure 4 (see also Appendix A).

The simple argument presented here attributes red shifts in ν_{CN} to changes in CN$^-$ bond order. We find nothing in the experimental observations that makes it necessary to postulate markedly different dπ/π* (or dπ/π) interactions for the C and N ends of CN$^-$. Of course there are differences in the Hückel treatment that arise from the different ionization energies of C and N, and from the differences in M/C and M/N coupling matrix elements, but these do not appear to be necessary to

(43) Carriedo, G. A.; Connelly, N. G.; Alvarez, S.; Perez-Carreño, E.; Garciá-Granda, S. *Inorg. Chem.* **1993**, *32*, 272.

Figure 5. Comparison of variations in ν_{CN} for some bridged complexes of low symmetry, mostly complexes of the type (PP)$_2$M(CNM′(NH$_3$)$_5$)$_2$. The parent bis(dicyano) complexes are indicated by an asterisk (*). All of the bridged complexes contain D/A pairs except for the Ru^{II}−(CN$^-$)−Rh^{III}, and the Ru^{II}−(CN$^-$)−Ru^{II} complexes. The latter are included to illustrate the commonly observed shift of ν_{CN} to higher frequencies when the metals bridged do not form a D/A pair. Results are also included for the Rh^{III}−(CN$^-$)−Ru^{II} complex, which indicate that very little shift of ν_{CN} is to be expected when the parent frequency is relatively high and the metals bridged do not form a D/A pair. Data are from Table 2.

account for the general patterns of shifts in ν_{CN}. The most important issue is properly accounting for the symmetry-allowed couplings (i.e., allowing for the nodal plane in the π* orbital). The smaller differences in interaction energies may also be important in some comparisons.

We have been unable to extend this type of argument to provide insight into the red shifts of ν_{CN} that occur when CN$^-$ bridges a donor and an acceptor. Most notably, the repulsive dπ/π interactions seem to dominate the behavior of monometal Cr(III) and Rh(III) cyanide complexes, but in the Ru(NH$_3$)$_5$$^{2+}$ metalates of the Cr(III) complexes we find a large red shift of ν_{CN}, while this is not observed for the Rh(III) complexes. The D/A systems require some features in addition to those in the simple perturbational treatment.

b. Shifts in ν_{CN} Complexes with Bridged Donors and Acceptors. The patterns of the shifts in ν_{CN} for low-symmetry D/A complexes are illustrated in Figure 5. We have included observations on Ru^{II}−(CN$^-$)−Ru^{II}, Ru^{II}−(CN$^-$)−Rh^{III} and Rh^{III}−(CN$^-$)−Ru^{II} complexes in Figure 5 to illustrate the contrasting behavior of ν_{CN} when the metals bridged do not form a D/A pair. It is especially in comparison to these complexes that the shifts of ν_{CN} to lower frequencies and the higher frequencies of ν_{CN} observed when the metals bridged do form a D/A pair are so dramatic. For example, the replacement of Rh(NH$_3$)$_5$$^{3+}$ by Ru(NH$_3$)$_5$$^{3+}$ results in a decrease in ν_{CN} by 80−100 cm^{-1} for the Ru^{II}−(CN$^-$)−Rh^{III} and Ru^{II}−(CN$^-$)−Ru^{III} complexes, and replacement of the central Rh-(III) by Cr(III) results in a decrease of about 70 cm^{-1} for the respective Rh^{III}−(CN$^-$)−Ru^{II} and Cr^{III}−(CN$^-$)−Ru^{II} complexes. These large decreases in ν_{CN} approximately correlate with the oscillator strength of the DACT absorption band, but there is no obvious correlation with simple local interactions such as electrostatic polarization[35] or donor/π*(CN$^-$) back-bonding. The qualitatively important feature of the behavior of ν_{CN} in bridged D/A complexes is that the size of the shift to lower frequency appears to increase with increases in the D/A "electronic" matrix element, β_{DA} (based on eq 1). These points are developed more carefully in the following.

The shifts of ν_{CN} can be interpreted in terms of variations in

the stretching force constant, k_{st}. Variations in k_{st} can come about because (a) there are variations in CN^- bond order (as argued in the previous section) and/or (b) the CN^- stretch contributes to the electron transfer coordinate, and there are changes in the shape of the ground state potential energy surface when there is strong D/A coupling (for V the potential energy, $k_{eff} = d^2V/dx^2$, where x is the relevant nuclear coordinate). The flattening of the ground state potential energy surface is a characteristic consequence of vibronic coupling.[44-46] A vibronic coupling model assumes that the electronic distribution is in equilibrium with the nuclear coordinates, and this has the qualitative effect of removing some electronic repulsions that inhibit motion along the reaction coordinate, e.g., this feature accounts for some observations on classical, halide-bridged (inner sphere) electron transfer reactions.[47] In the present context, this aspect of vibronic coupling has the effect of eliminating the repulsive component of the $d\pi-(\pi^*,\pi)-d\pi$ interaction, so that the resulting $D-(CN^-)-A$ interaction can be interpreted as being dominated by back-bonding (*vide infra*). After making note of some additional features of the experimental observations, we will develop a simple vibronic model to account for the shifts in ν_{CN}.

As noted in Table 2, large red shifts are observed when a donor and an acceptor are bridged by CN^-. For perspective, it is useful to note that the difference between the typical CN stretching frequencies for triple- and double-bonded CN moieties is approximately 500 cm^{-1} [48] and that a unit change in bond order corresponds approximately to a 23×10^3 cm^{-1} decrease in bond energy.[49] As noted earlier, the referencing of the shifts in ν_{CN} for such discussions is somewhat equivocal. However, the full range observed for ν_{CN} in CN^--bridged complexes is more than 100 cm^{-1} or about 20% of the change associated with a one unit decrease in bond order. It is most striking that ν_{CN} for $Rh^{III}-(CN^-)-Ru^{II}$ is at the high end of its range, while ν_{CN} for $Cr^{III}-(CN^-)-Ru^{II}$ is nearer the low-frequency end. No simple back-bonding model can account for the direction of this shift. Although Co(III) is the stronger oxidant (by roughly 1 V), the arguments presented earlier suggest that the much lower frequency observed for ν_{CN} in $Cr^{III}-(CN^-)-Ru^{II}$ than in $Co^{III}-(CN^-)-Ru^{II}$ complexes implies a greater amount of charge delocalization in the Cr(III) complex. This specific example of a point made at the beginning of this section illustrates that D/A coupling must involve both electronic and nuclear components.

B. A Simple Vibronic Model for Coupling a Bridging CN^- with an Electron-Transfer Donor and Acceptor in $d\pi$ (π, π^*) $d\pi$ complexes. Vibronic models for simple electron transfer systems have been discussed by Peipho, Krausz and Schatz,[50] Peipho,[51] and Ferretti *et al.*[52] While these approaches have focused primarily on the CT spectroscopy of the Creutz–Taube ion,[53] they involve conceptual approaches that are similar

to that employed here. The approach of Ferretti *et al.* is conceptually most similar to ours, in that it implicates CT excited states of the bridging ligand (MLCT and LMCT states) in the propagation of DA coupling. We have developed an approach that allows us to use spectroscopic parameters, which are measurable in principle, to evaluate the effects of vibronically propagated DA coupling on several properties of the DA complex.[10,13,33,47] The vibronic model makes the fundamental assumption that the electronic and nuclear coordinates are in equilibrium on the time frame in question,[54] so that the CN^- stretching motion would encounter little or no repulsion from the $d\pi$ electrons of bridged donor and acceptor, and β_{DA} would be a function of the nuclear coordinates. This situation can be represented by expressing the D/A coupling matrix element and the potential energies of the ground and excited state electron transfer states as linear functions of the electron transfer coordinate, x (in the present systems, this is coincident with the CN^- bond), as in eqs 4 (see Appendix B).[44-47,51,52] The

$$\beta_{DA} \cong \beta_{DA}{}^\circ + bx \qquad (4a)$$

$$V_D \cong V_D{}^\circ + kx^2/2 - ax \qquad (4b)$$

$$V_A \cong V_A{}^\circ + kx^2/2 + a'x \qquad (4c)$$

linear terms in the potential energy functions (ax and $a'x$) arise from local metal–cyanide interactions (i.e., contributions of ligand-to-metal and metal-to-ligand CT perturbations), for which the corresponding LMCT and MLCT excited states have potential energy minima that are displaced with respect to that of the ground state (Appendix B).[13] The nuclear coordinate dependence of β_{DA} can also be expressed as a power series, and eq 4a neglects any higher order terms in the power series expansion (see the analogous treatments of Jahn–Teller effects[44-46] and Appendix B).

The $V_i{}^\circ$ in eqs 4b and 4c represent the vertical potential energies (evaluated at $x = 0$), and, as a result of our definitions, $V_A{}^\circ$ differs from the potential energy at the diabatic minimum by an amount $kr_o{}^2/2 + \epsilon_{ACT}{}^\circ$, and $a' \cong a - kr_o + \alpha_{CT}{}^2kr_o$ (Appendix B). To simplify this discussion, we have set $a' \cong a$. We further define $E_{DA}{}^\circ = V_A{}^\circ - V_D{}^\circ$. Since the quadratic terms in eqs 4b and 4c have the same sign, they do not need to be considered explicitly in the secular determinant, which can then be formulated as in eq 5 (x in these equations represents

$$\begin{vmatrix} -ax - \epsilon & \beta_{DA}{}^\circ + bx \\ \beta_{DA}{}^\circ + bx & E_{DA}{}^\circ + ax - \epsilon \end{vmatrix} = 0 \qquad (5)$$

a generalized electron transfer coordinate). The solutions of eq 5 describe the adiabatic ground and excited electron transfer states, which result from the vibronic coupling. The resulting adiabatic potential energy functions are given by eq 6. For small

$$V_\pm \cong kx^2/2 + E_{DA}{}^\circ/2 \pm {}^1/_2[E_{DA}{}^{\circ 2} + 4axE_{DA}{}^\circ + 4a^2x^2 + 4(\beta_{DA}{}^\circ + bx)^2]^{1/2} \qquad (6)$$

x, and for $E_{DA}{}^{\circ\,2} \gg [4axE_{DA}{}^\circ + 4a^2x^2 + 4(\beta_{DA}{}^\circ + bx)^2]$, the ground state potential function is represented by eq 7. The

(44) Bersuker, I. B. *The Jahn-Teller Effect and Vibronic Interactions in Modern Chemistry*; Plenum: New York; 1984.

(45) Fischer, G. *Vibronic Coupling*; Academic: New York, 1984.

(46) Ballhausen, C. J. In *Vibronic Processes in Inorganic Chemistry*; Flint, C. D., Ed.; Kluwer Academic Publishers: Dordrecht, 1989; p 53.

(47) Schwarz, C. L.; Endicott, J. F. *Inorg. Chem.* **1995**, *34*, 4572.

(48) Drago, R. S. *Physical Methods*; Saunders: Philadelphia, 1992; p 187.

(49) Huheey, J. E. *Inorganic Chemistry*, 3rd ed.; Harper and Row: Philadelphia, 1983; p A-37.

(50) Piepho, S. B.; Krausz, E. R.; Schatz, P. N. *J. Am. Chem. Soc.* **1979**, *100*, 2996.

(51) (a) Piepho, S. B. *J. Am. Chem. Soc.* **1988**, *110*, 6319. (b) Piepho, S. B. *J. Am. Chem. Soc.* **1990**, *112*, 4197.

(52) Ferretti, A.; Lanie, A.; Ondrechen, M. J.; Villani, G. *J. Phys. Chem.* **1995**, *99*, 10484.

(53) (a) Creutz, C.; Taube, H. *J. Am. Chem. Soc.* **1969**, *91*, 3988. (b) Creutz, C.; Taube, H. *J. Am. Chem. Soc.* **1973**, *95*, 1086.

(54) This assumption is consistent with the usual Born–Oppenheimer approximation that electronic relaxation is rapid on the time scale for nuclear motion. However, this is in contrast to a fundamental assumption of most nonadiabatic electron transfer theories: that the electron "jumps" only after nuclear rearrangement has taken place. The latter is equivalent to the CBOA mentioned in the Introduction.

Figure 6. Qualitative potential energy surfaces illustrating the effects of vibronic coupling between a donor and an acceptor. The figure illustrates the successive steps of a simple model for vibronic coupling: (a) the perturbational mixing of a CT excited state (a composite of MLCT and LMCT states involving the bridging ligand) with diabatic electron transfer ground (D) and excited (A) states before CT coupling (solid line represents the effect of the vertical CT coupling perturbation); (b) the effect of vibronic perturbation coupling (solid line) of the CT perturbed electron transfer ground and excited state PE surfaces generated in (a) (dashed line). Vertical dotted lines are drawn to the minima of the diabatic surfaces in (a) to facilitate comparison. Some of the energy difference between the diabatic curves and the CT-perturbed curves in (a) is correlated with the net charge delocalized from D to A as a consequence of the local CT perturbations and can be regarded as an important contribution to $\beta_{DA}°$.

effects of vibronic coupling are (a) to displace the potential

$$V_- \cong kx^2/2 - \beta_{DA}°^2/E_{DA}° - x(a + 2\alpha_{DA}°b) -$$
$$x^2(a^2 + b^2)/E_{DA}°$$
$$\cong kx^2/2 - ax - 2\alpha_{DA}°bx \qquad (7)$$

energy minima along the x coordinate (see eq 8), (b) to flatten the ground state PE surface (see eq 9), and (c) to produce the large separation of the ground and excited state surfaces characteristic of an adiabatic system (see Figure 6). These effects are illustrated qualitatively in Figure 6. The displacement of the ground state surface can be evaluated on the basis of $(dV_-/dx) = 0$, as in eq 8. This is not an important issue in the present report, and the significance of this displacement on ϵ_S is considered elsewhere.[13b]

$$x_{min} \cong (a + 2\alpha_{DA}°b)/k \qquad (8)$$

Similarly, the separation of V_- and V_+ is not a major concern in the present report. The issue of concern here is the effect of vibronic coupling on the effective CN⁻ stretching force constant, k_{st}. If displacements of the bridging C and N atoms are major components of the electron transfer coordinate x, then k_{st} may

be assumed to be proportional to k_{eff}, where $k_{eff} = d^2V_-/dx^2$. Thus, from eq 8, and from evaluating the derivative function at $x \cong 0$, we find an expression for the effective force constant given by eq 9. Clearly, when vibronic coupling is important, $k_{eff} < k$, and by inference there is a proportional decrease in k_{st}.

$$k_{eff} \sim k - 2(a^2 + b^2)/E_{DA}° \qquad (9)$$

The parameters a and b in eq 9 are linear vibronic constants,[44−46] whose magnitudes determine the relative importance of vibronic coupling. By combining eq 7 and 8, one obtains eq 10, which expresses the dependence of the ground

$$\epsilon_s{}^{th} \cong \beta_{DA}°^2/E_{DA}° + k(x_{min})^2/2 \qquad (10)$$

state stabilization energy, $\epsilon_s{}^{th}$, on the vibronically induced displacement of the ground state PE surface (see Figure 6). The first term in eq 10 is the vertical perturbation term, which is normally considered[2,3] in treatments of CT interactions.

Equation 10 might be used as the basis for exploring the apparent rough correlation of $\Delta\nu_{CN}$ with DACT oscillator strength, but we have found this approach to be algebraically complex. It is somewhat simpler to consider the electronic matrix element inferred from the optical measurements and eq 1. Thus, the experimental matrix element can be defined as in eq 11. We see that the same parameters are involved in eqs 9
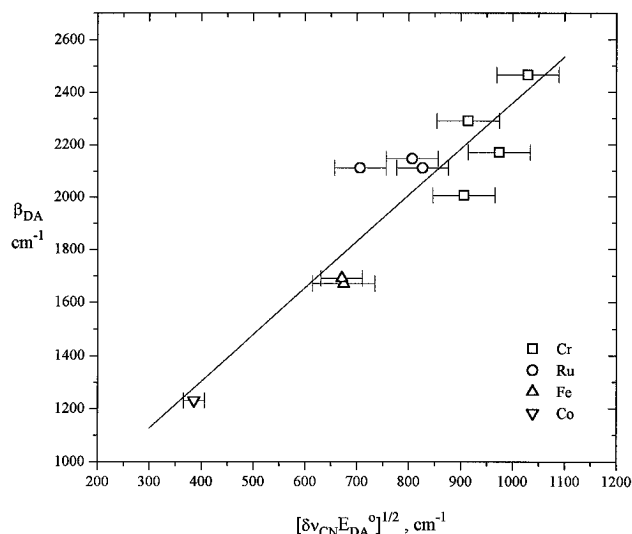
$$\beta_{DA}{}^{expt} \cong \beta_{DA}° + bx_{min} \cong \beta_{DA}° + (a + 2\alpha_{DA}°b)(b/k) \quad (11)$$

and 11. Since a is the product of a mixing coefficient ($\alpha_{CT} = \beta_{CT}°/E_{CT}°$) and a reorganizational factor, and since b does not contain the corresponding mixing coefficient (α_{DA}; see Appendix B), one expects $a^2 \ll b^2$. As a result, eq 9 can be reexpressed as $b^2 \cong \Delta\nu E_{DA}°k/\nu$, where $\Delta\nu$ is the frequency shift of the coupled vibrational motions whose effective frequency is ν. Substitution into eq 11 leads to a relatively simple relationship, eq 12, between the shift in the frequency of the

$$\beta_{DA}{}^{op} \cong \beta_{DA}° + (a/\sqrt{k})(\Delta\nu E_{DA}°/\nu_{eff})^{1/2} + 2(\Delta\nu/\nu)\beta_{DA}°$$
$$(12)$$

coupled vibrational motion, $\Delta\nu$, and the D/A coupling matrix element, $\beta_{DA}{}^{op}$, inferred from the observed absorption spectrum. The parameters $\Delta\nu$ and ν inferred from this simple classical argument should be interpreted as composites (or the means) of contributions from all of the coupled nuclear motions in the $(Dd\pi)-(CN⁻)-(Ad\pi)$ systems considered in this section. The redistribution of charge is expected to result in relatively small changes in frequency associated with the internal vibrations of D and A (all skeletal modes are low-frequency vibrations, and bond length changes are expected to be very small). The substantial red shifts in $\Delta\nu_{CN}$ that have been discussed here and the enhanced CN⁻ vibrations found in the resonance Raman of some related complexes[55] indicate that the CN⁻ stretch must be among the contributing vibrations, and it is plausible to assume that $\Delta\nu_{CN}$ is proportional to $\Delta\nu$; i.e., $\Delta\nu_{CN} = \gamma\Delta\nu$, where γ is a constant determined by the fractional weight of the ν_{CN} contribution to λ_{DA}. The numerical value of the frequency ν to be used in eq 12 is not obvious,[55] and some of the contribution to ν must arise from solvational changes at the pentaammine moieties. Consequently, we have not attempted to assign values for ν in our evaluation of eq 12.

(55) For example, resonance Raman studies of related $(CN)_5$-$Ru(CNRu(NH_3)_5)^-$ complexes have implicated several vibrational contributions to λ_{DA} in these complexes: Doorn, K. S.; Hupp, J. T. *J. Am. Chem. Soc.* **1989**, *111*, 1142.

Figure 7. Correlation of the red shift of the CN⁻ stretching frequency with the apparent electronic coupling between the donor and acceptor, $\beta_{DA}°$, in bridged D/A complexes. Based on the first term on the right-hand side of eq 14. The "red" shift, $\Delta\nu_{CN}$, is based on the average frequencies of the symmetric and antisymmetric in complexes with C_2 symmetry, except for (bpy)₂Ru(CNRu(NH₃)₅)₂⁶⁺ for which the lowest energy component was used. Data for C_2 and lower symmetric complexes have been used and are from Table 2.

Finally, $\beta_{DA}°$ cannot be a constant through the series of compounds employed here. However, for the (Ddπ)−(CN⁻)−(Adπ) complexes, one expects that the corresponding oscillator strengths and bandwidths (here, these correspond to an extrapolation to $x = 0$ and the CT mixing corresponding to this nuclear configuration) will be roughly comparable, so that the variations in $\beta_{DA}°$ will be roughly proportional to $(E_{DA}°)^{1/2}$ (see eq 1). Thus, the correlation of experimental parameters can be examined by using eq 13 (formally, A is a collection of terms:

$$\beta_{DA}{}^{op} \cong A + B\delta\nu_{CN}\sqrt{E_{DA}°\nu_{CN}} \qquad (13)$$

$\beta_{DA}°$ and other terms from eq 12; see Appendix C). The resulting correlation (Figure 7) is reasonably good in view of the approximations and simple classical argument used to obtain eq 13. Figure 7 emphasizes the qualtiative point made earlier: namely, the red shifts of ν_{CN} found when CN⁻ bridges a donor and acceptor *are a function of the electronic coupling between the donor and acceptor*. This observation must be regarded as strong evidence for vibronic coupling.

C. Donor−Acceptor Coupling in dπ−(π,π^*)dσ Systems. The preceding vibronic arguments are based on the coupling of dπ donors to dπ acceptors through the π/π^* network of CN⁻. We have included several systems with dσ acceptors and dπ donors in Table 2 and one in Figure 7. Since electron transfer coupling is formally z allowed, and since any dσ/dπ coupling in a rigid, linear system is x, y allowed, one would expect the charge delocalization along the z axis of these systems to be less than what might be inferred by the naive application of eq 1 to their DACT absorption spectra. These systems are important in the present discussion in helping to define the limit of β_{DA} as $x \rightarrow 0$ (i.e., $\beta_{DA}° \leq 500$ cm⁻¹), since the Co^{III}−(CN⁻)−Ru^{II} systems involve a d$\pi \rightarrow$ dσ transition.

We do note that symmetry issues are a matter of concern in these systems. Thus, we have shown that they must be taken into account in the interpretation of parameters obtained from eqs 1 and 2: (a) in comparing *cis*- and *trans*-diruthenates to monoruthenates and (b) in treating the interactions of dπ donors with a π-bridging ligand and in determining which vibrational modes are important in vibronic coupling.

Conclusions. Examination of variations in the CN⁻ stretching frequencies of several series of transition metal dicyanide complexes has revealed some important features of the electronic interactions in these complexes:

1. The importance of M $\rightarrow$ CN⁻ back-bonding is manifested by red shifts of ν_{CN} in the monometal parent complexes.

2. When CN⁻ serves as a bridging ligand between two metals that are not a donor−acceptor pair, ν_{CN} shifts to higher energies. This blue shift is observed even when each of the bridged metals is able to participate in back-bonding. This is apparently the consequence of electronic repulsions, which can be viewed as arising either from cancellation of the charge delocalization associated with coupling when it is symmetry adapted or from the repulsion between back-bonding of two donors to the out-of-phase orbital components of the π^*(CN⁻) orbital.

3. When CN⁻ bridges a donor and an acceptor, ν_{CN} red shifts by very substantial amounts. The red shift does not correlate with M $\rightarrow$ CN⁻ back-bonding, but it does correlate with the oscillator strength of the donor−acceptor charge transfer absorption.

4. The vibrational modes that are important in vibronic coupling appear to be those required by simple symmetry selection rules. The much greater red shift of ν_s than of ν_a in *trans*-Cr([14]aneN₄)(CNRu(NH₃)₅)₂⁵⁺ is the first demonstration of the *symmetry dependent* coupling between bridging ligand vibrational modes and the donor and acceptor electronic wave functions.

5. A simple vibronic mechanism can accout for the influence of D/A coupling on the C−N stretching frequency.

Appendix A. A Hückel-like Treatment of Metal Cyanide π Interactions

Because C/N π bonding is so strong relative to dπ/π^*(CN⁻) or π(CN⁻)/dπ π bonding, the interactions can be treated perturbationally. However, this is a three-center problem. For simplicity, we consider the interactions between the dπ(M), π-(C), and π(N) atomic orbitals in a single plane. The secular equation[44] can be written as in eq A1, in which we have considered only the nearest neighbor couplings (β_1 for C/N and β_2 for M/C). Δ is the energy difference of the dπ and pπ

$$-\epsilon^3 + \epsilon^2\Delta + (\beta_1{}^2 + \beta_2{}^2)\epsilon - \beta_1{}^2\Delta = 0 \qquad (A1)$$

orbitals, and we have assumed that pπ(C) and pπ(N) have similar energies. For weak M/CN⁻ π interactions, the perturbational solutions of the cubic equation may be obtained by considering in turn the equations generated by setting $\epsilon_\pi = \beta_1 + \delta_\pi$, $\epsilon_{\pi^*} = -\beta_1 + \delta_{\pi^*}$ and $\epsilon_M = \Delta + \delta_M$. For $\beta_1{}^2 > (\Delta^2,\beta_2{}^2) > \delta_i{}^2$, only terms first order in δ_i need to be considered (this is equivalent to the limit in which $\Delta = 0$), and the first-order solutions of $\delta_\pi = \beta_2{}^2/2\beta_1 = -\delta_{\pi^*}$, and $\delta_M = 0$ are obtained. When $|\Delta| > 0$ (as for a relatively ionizable metal), second-order corrections must be considered. If only terms first and second order in δ_i are considered, and if the orbital center of gravity is maintained, the second-order correction terms are of the form given in eq A2. This limit corresponds to that of a

$$\left.\begin{array}{l} \delta_\pi = (\beta_2{}^2/2\beta_1{}^2)\Delta \\ \delta_\pi{}^* = (\beta_2{}^2/2\beta_1{}^2)\Delta \\ \delta_M = -(\beta_2{}^2/\beta_1{}^2)\Delta \end{array}\right\} \qquad (A2)$$

"back-bonding" metal. When a $d\pi/\pi(CN^-)$ bonding perturbation is important, the sign of Δ is changed. However, since Δ is the difference in d(M)- and p(C,N)-orbital ionization energies, its sign does not depend on an assumption about the nature of the net bonding interaction. Since the $d\pi(Ru(NH_3)_3{}^{2+}) \rightarrow \pi^*(CN^-)$ MLCT and the $\pi(CN^-) \rightarrow d\pi(Ru(NH_3)_5{}^{3+})$ LMCT transitions occur in the range $(30-40) \times 10^3$ cm^{-1},[13] $|\Delta|$ cannot be very large for Ru(NH$_3$)$_5{}^{2+}$. Thus, for a difficult to ionize d^6 metal, such as Rh(III), a negative value for Δ is plausible, and the resulting $d\pi(Rh)/\pi(CN^-)$ interaction is best described as a repulsion.

Pertinent to the overall argument in this paper, the first-order terms have the form of the stabilization energies expected of MLCT, for $\beta_2{}^2/(\beta_1 - \Delta)$, and of LMCT, for $\beta_2{}^2/(\beta_1 + \Delta)$, for perturbational mixing of these excited states with the ground state (and taking account of orbital occupations). The second-order corrections are of the form $(\beta_2{}^2/\beta_1{}^2)\Delta$, and $\beta_2{}^2/\beta_1{}^2 = \alpha^2$ is readily interpreted as the fraction of charge delocalized. Consequently, the second-order terms that appear in expressions for the corrected state energies can be readily interpreted as arising from the changes in bond order that result from charge delocalization. These effects of charge delocalization, which appear as second-order terms in the Hückel-like perturbation treatment presented here, are postulated to be important in the bridging ligand's propagation of D/A coupling, as well as in changes in vibrational frequencies. This argument can readily be extended to dicyano complexes. The extension to centrosymmetric complexes will be discussed elsewhere.[33]

Appendix B. Some Details of Terms Employed in the Vibronic Argument

Some of the terms and approaches are described here. A more detailed discussion will be presented elsewhere.[13] If the diabatic PE minimum has an energy $V_D{}^\circ$, then $V_D = V_D{}^\circ + k(r_o - x)^2/2 + \epsilon_{DACT}{}^\circ$, where r_o is the horizontal displacment between the electron transfer ground and excited state PE surfaces and $\epsilon_{DACT}{}^\circ$ is a combination of LMCT and MLCT stabilizations of the electron transfer excited state evaluated at $x = 0$. A first-order Taylor series expansion of ϵ_{DACT} around $x = 0$ is of the form[13] $\epsilon_{DCT} \cong \epsilon_{DCT}{}^\circ + \alpha_{CT}{}^\circ a x - (\alpha_{CT}{}^\circ)^2 r_o x$, where $\alpha_{CT}{}^\circ = \beta_{DCT}/E_{DCT}{}^\circ$, $\beta_{DCT} \cong \beta_{DCT}{}^\circ + b_{CT}$, and $E_{DCT}{}^\circ$ is the mean energy difference between the diabatic electron transfer ground state (D) and the MLCT/LMCT excited states. In the following argument, we have assumed that $\beta_{ACT}{}^\circ \cong \beta_{DCT}{}^\circ = \beta_{CT}{}^\circ$ and $E_{ACT}{}^\circ \sim E_{DCT}{}^\circ = E_{CT}{}^\circ$, where the subscript A designates the electron transfer excited state.

We show elsewhere[13] that for the parameters defined earlier, $a \cong \alpha_{CT}{}^\circ \sqrt{k\lambda_{CT}/2}$ and $b \cong \sqrt{k\lambda_{DA}/2}$, where $\alpha_i{}^2$ and λ_i are the fraction of the charge delocalized and the nuclear reorganizational energy per unit of charge for the designated first-order charge transfer couplings, respectively ($i = CT$ and DA, respectively, for the average of MLCT and LMCT couplings and for the D/A coupling); $\alpha_i{}^\circ = \beta_i{}^\circ/E_i{}^\circ$.

When the electronic wave function is a function of both the electronic and nuclear coordinates, as in the Born–Oppenheimer approximation, then the D/A electronic matrix element in principle can be expanded around the coupled nuclear displacement coordinates (represented by x), and it is usually assumed that only the first term in this expansion need be considered.[44−46] A simple, nonrigorous way of obtaining eq B1 is to assume

$$\beta_{DA} = \beta_{DA}{}^\circ + bx + b'x^2 + ... \qquad (B1)$$

that D/A coupling can be represented as an exponential function of the displacement parameter x, so that expansion around x gives eq B1. The coefficient b can be evaluated by considering the symmetrical ($\Delta G^\circ = 0$), weakly coupled limit ($\beta_{DA}{}^\circ \sim 0$) and substituting the appropriate quantities from standard electron transfer theory.[13] Essentially the same result is obtained from the relationship between linear vibronic constants and the Huang−Rhys factor.[46]

Appendix C. Some Details of the Correlation between β_{DA} and $\Delta\nu$ Based on the Simple Vibronic Model

The linear vibronic constants can be related to the appropriate force constants and reorganizational parameters, as in eqs C1 and C2 (see also Appendix B), where $\alpha_{CT}{}^\circ = \beta_{CT}{}^\circ/E_{CT}{}^\circ$ for

$$a \cong 4\alpha_{CT}{}^\circ[\lambda_{CT}k_{CT}/2]^{1/2} \qquad (C1)$$

$$b \cong [\lambda_{DA}k_{DA}/2]^{1/2} \qquad (C2)$$

the perturbing CT excited state [$\beta_{CT}{}^\circ$ is the couplng matrix element, $E_{CT}{}^\circ$ is the vertical energy difference between ground state and CT excited state PE surfaces, and k_i and λ_i are the force constants and reorganizational energies associated with the ground state to LMCT/MLCT ($i = $ CT) and DACT ($i = $ DA) electron transfer transitions, respectively].[13] We have assumed $k_i = k$. The factor of 4 in eq C1 arises from (a) the sum of contributions (assumed to be equal) of LMCT and MLCT stabilization energies and (b) the first-order term in the Taylor series expansion of ϵ_{CT} around $x = 0$, assuming that $\beta_{CT} \cong \beta_{CT}{}^\circ + b_{CT}x$ (as in eq 6a) and that $\epsilon_{CT} = (\beta_{CT})^2/E_{CT}$. On the basis of these assumptions, a^2 is typically much smaller than b^2 (α_{CT} is typically less than 0.1), and b^2 can be evaluated from eq 11 as in eq C3. For a normal vibrational mode, $k = 4\pi^2\mu\nu^2$

$$b^2 \cong E_{DA}{}^\circ(k - k_{eff})/2 \qquad (C3)$$

(μ is the effective mass). If we set $k_{eff} \cong 4\pi^2\mu(\nu - \Delta\nu)^2 \cong 4\pi^2\mu[\nu^2 - 2\nu\Delta\nu]$, then substitution into eq C3 gives eq C4,

$$b^2 \cong E_{DA}{}^\circ\Delta\nu/k\nu \qquad (C4)$$

which can be substituted into eq 13 to obtain eq 14. Since both terms on the right-hand side of eq 11 contain a mixing coefficient (α_i), their relative weight is not immediately obvious. Consideration of the DACT, M $\rightarrow$ CN$^-$ MLCT, and CN$^-$ $\rightarrow$ M′ LMCT absorption bands in typical $d\pi/d\pi'$ complexes[13] indicates that $\alpha_{CT}{}^\circ$ is typically less than twice as large as $\alpha_{DA}{}^\circ$ and that $\lambda_{CT} \sim 2\lambda_{DA}$. Such values for these parameters imply that $ab/\alpha_{DA}{}^\circ b^2 \sim 4\sqrt{2}$, so that the first term would be expected to make a somewhat larger contribution. We have based the correlation in Figure 7 on this term. Other functions of the type $(\Delta\nu_{CN})^m(E_{DA}{}^\circ)^n$ (m, n = 1 or $^1/_2$) also give plausible correlations. For these reasons, as well as the uncertainties in the evaluation of $\Delta\nu_{CN}$, Figure 7 should be regarded as an empirical correlation. While the slope of this correlation currently cannot be regarded as particularly meaningful, it is certainly plausible. Values mentioned earlier for parameters in the first term on the right-hand side of eq 14 suggest a slope greater than about 0.8 (ν is a composite frequency of less than 2×10^3 cm^{-1}), and the observed slope is about 2.